

A Study on the Seismic Isolation Systems of Bridges with Lead Rubber Bearings

Woo-Suk Kim, Dong-Joon Ahn, Jong-Kook Lee*

School of Architecture, Kumoh National Institute of Technology, Gumi, Republic of Korea
Email: kimw@kumoh.ac.kr, djahn@kumoh.ac.kr, ljk@kumoh.ac.kr

Received 12 September 2014; revised 8 October 2014; accepted 28 October 2014

Copyright © 2014 by authors and Scientific Research Publishing Inc.
This work is licensed under the Creative Commons Attribution International License (CC BY).
<http://creativecommons.org/licenses/by/4.0/>



Open Access

Abstract

This study consists of the development and presentation of example of seismic isolation system analysis and design for a continuous, 3-span, cast-in-place concrete box girder bridge. It is expected that example is developed for all Lead-Rubber Bearing (LRB) seismic isolation system on piers and abutments which placed in between super-structure and sub-structure. Design forces, displacements, and drifts are given distinctive consideration in accordance with Caltrans Seismic Design Criteria (2004). Most of all, total displacement ($D_{TM} = 457$ mm) on design for all LRBs case is reduced comparing with combined lead-rubber and elastomeric bearing system ($D_{TM} = 533$ mm). Therefore, this represents substantial reduction in cost because of reduction of expansion joint. This presents a summary of analysis and design of seismic isolation system by energy mitigation with LRB on bridges.

Keywords

Seismic Isolation System, Bridge, Lead Rubber Bearing (LRB), Energy Mitigation

1. Introduction

Seismic isolation systems are the separating of structures (such as bridge, building, railway, road, airport, harbor, dam, and tunnel etc.) from ground motions generated by earthquakes which could induce damage to the structures. Among various seismic isolation systems, lead-rubber bearing (LRB) which has innovative mechanism can lead to increased effective stiffness and is accommodating force in reinforced concrete (RC) structures. LRB is a novel apparatus based on the combination of laminated layers rubber bearing using lead plugs (Constantinou, *et al.* (2006) [1]). In this research, a bridge was selected to demonstrate the application of analysis and bearing

*Corresponding author.

design procedures for seismic isolation system. The bridge was used as an example of bridge design without an isolation system in the Federal Highway Administration (FHWA) Seismic Design Course, Design Example No. 4, prepared by Berger/Abam Engineers (1996) [2]. The bridge is a continuous, three-span, cast-in-place concrete box girder structure with a 30-degree skew. The two intermediate bents consist of two round columns with a crossbeam on top. The geometry of the bridge, section properties and foundation properties are assumed to be the same in the original bridge in the FHWA example (2000) [3]. It is presumed that the original bridge design is sufficient to sustain the loads and displacement demands when seismically isolated as described herein. Only minor changes in the bridge geometry were implemented in order to facilitate seismic isolation.

2. Description of Bridge

Figures 1-3 show, respectively, the plan and elevation, the abutment sections and a section at an intermediate bent. In Figure 3, the bent is shown at the skew angle of 30 degrees, whereas for the box girder the section is perpendicular to the longitudinal axis. The actual distance between the column centerlines is 7.92 m (Figure 1).

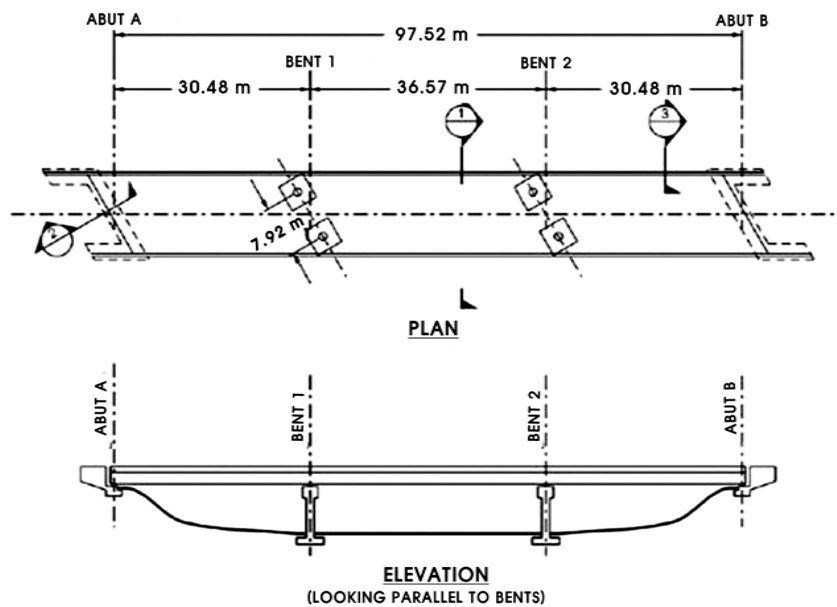


Figure 1. Bridge plan view and elevation.

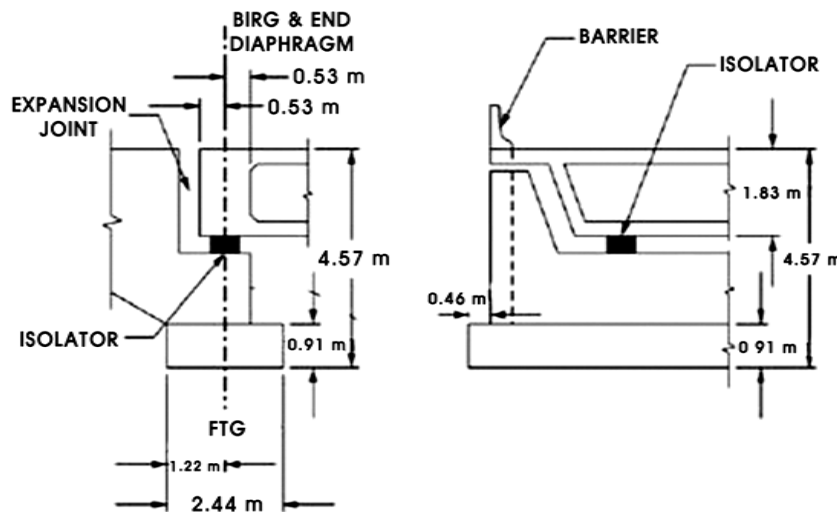


Figure 2. Section at abutment.

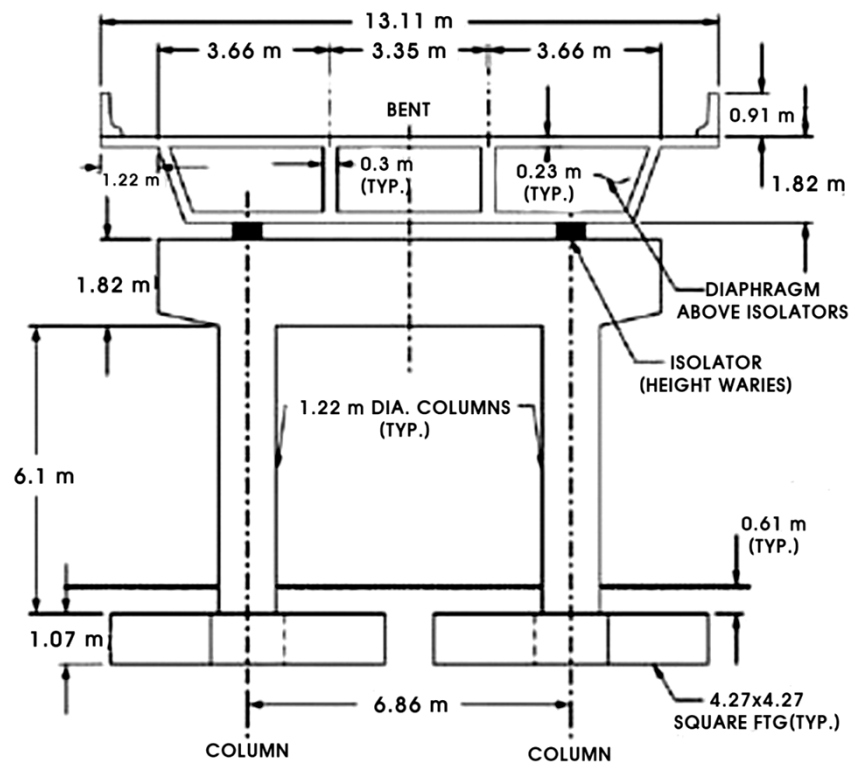


Figure 3. Cross section at intermediate bent.

The bridge is isolated with two multi-directional seismic isolators at each abutment and pier location for a total of eight multi-directional seismic isolators with lead rubber bearings. The isolators are directly located above the circular columns. The plan views of the isolated bridge are shown in [Figure 4](#).

The bridge is isolated with two isolators at each abutment and pier location for a total of eight isolators. The isolators are directly located above the circular columns. The use of two isolators versus a larger number is intentional for the following reasons:

- With elastomeric bearings it is possible to achieve a larger period of isolation (more mass per bearing).
- The distribution of load on each isolator is accurately calculated. The use of more than two isolators per location would have resulted in uncertainty in the calculation of the axial load in vertically stiff bearings.
- Reduction in construction cost.

For better distribution of load to the bearings, diaphragms are included in the box girder at the abutment and pier locations above the isolators. An additional 596 kN weight at each diaphragm location is introduced by the addition of these diagrams. The bridge is considered to have three traffic lanes. Loadings were determined based on AASHTO LRFD Specifications (2001) [4] with live load consisting of truck, lane and tandem and wind load being representative of typical sites in the Western United States.

[Figure 5](#) shows a model for the analysis of the bridge. The model may be used in static and multimode analysis.

The cross sectional properties of the bridge and weights are presented in [Table 1](#). The modulus of elasticity of concrete is $E = 24.82 \text{ GPa}$. Foundation spring constants are presented in [Table 2](#).

2.1. Analysis of Bridge for Dead, Live, Brake and Wind Loadings

The weight of the seismically isolated bridge superstructure is 22,650 kN. The difference is due to the presence now of diaphragms at the abutment and pier locations in order to transfer loads to the bearings. Kim (2007) [5] presents calculations for the bearing loads and rotations due to dead, live, braking and wind forces. [Table 3](#) presents a summary of bearing loads and rotations. On the basis of the results in [Table 3](#), the bearings do not experience uplift or tension for any combination of dead and live loadings.

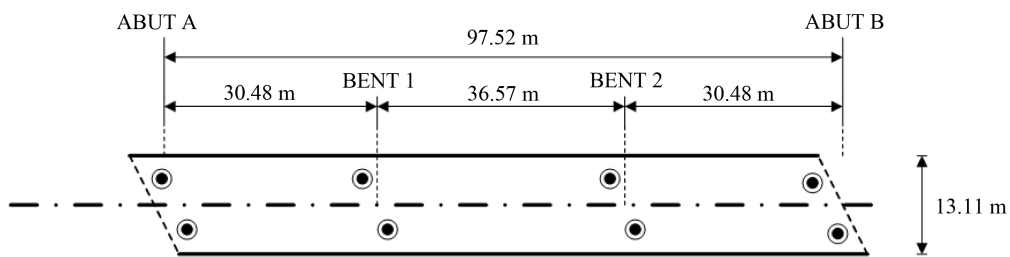


Figure 4. Plan view of bridge isolated with lead-rubber bearings.

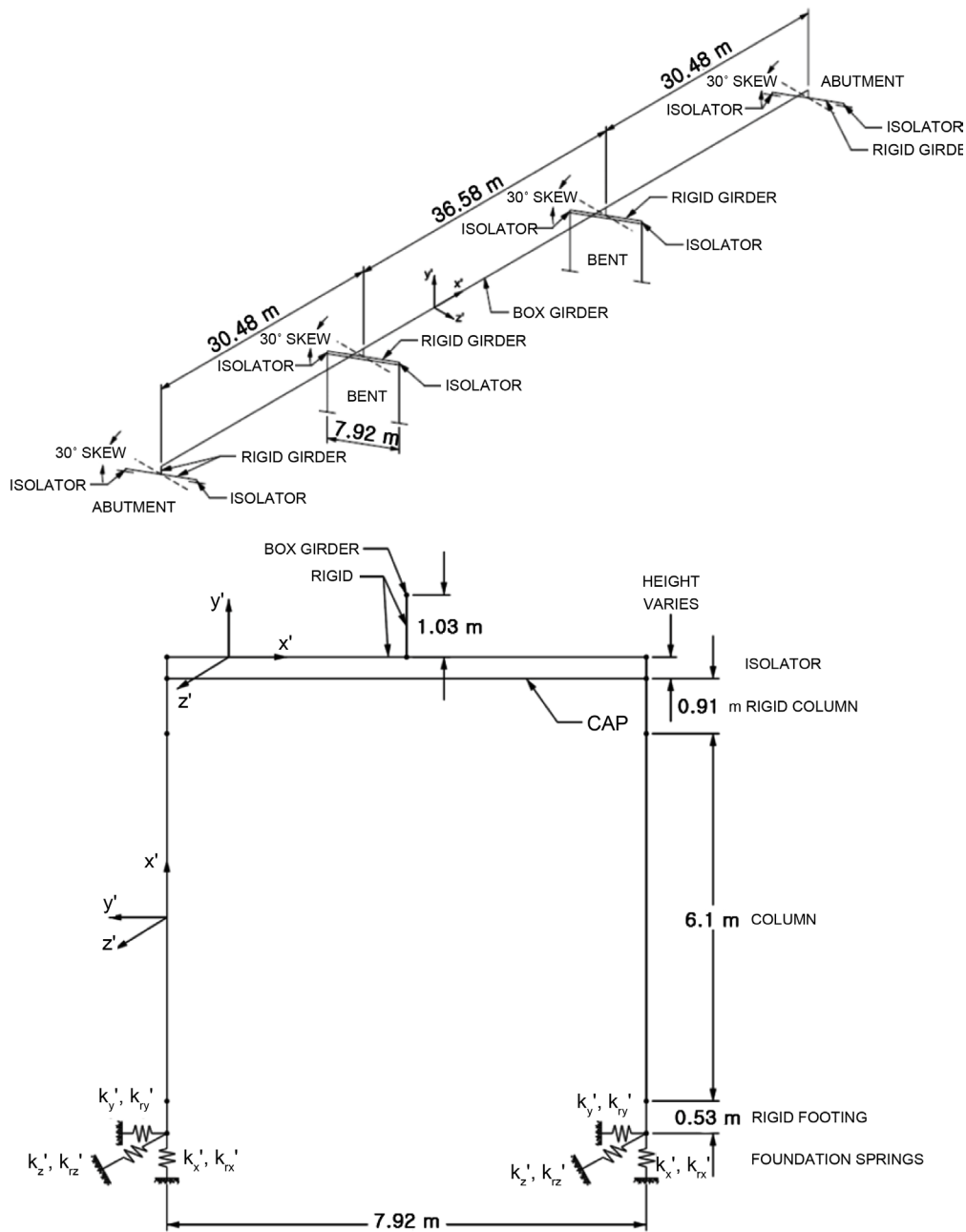


Figure 5. Model of bridge for single- and multimode analysis.

Table 1. Cross sectional properties and weights in bridge model.

Element Property	Box Girder	Bent Cap Beam	Column	Rigid Girder	Rigid Column	Rigid Footing
Area A_x^* (m ²)	6.76	2.23	1.17	18.58	18.58	18.58
Shear Area A_y^* (m ²)	2.25	2.23	1.17	18.58	18.58	18.58
Shear Area A_z^* (m ²)	5.30	2.23	1.17	18.58	18.58	18.58
Moment of Inertia I_y (m ⁴)	82.82	0.27	0.08**	854.07	854.07	854.07
Moment of Inertia I_z (m ⁴)	3.42	0.61	0.08**	854.07	854.07	854.07
Torsional Constant I_x (m ⁴)	15.12	0.64	0.21	854.07	854.07	854.07
Weight (kN/m)	207.9***	76.8	27.6	0	0	858.4****

*: Coordinates X, Y and Z refer to the local member coordinate system; **: Cracked section properties (0.7 I_g); ***: Add 596 kN concentrated weight at each bent and abutment location; ****: Total weight of footing divided by length of 0.53 m.

Table 2. Foundation spring constants in bridge model.

Constant	K_x (kN/m)	K_y (kN/m)	K_z (kN/m)	K_{rx} (kN-m/rad)	K_{ry} (kN-m/rad)	K_{rz} (kN-m/rad)
Description	Vertical stiffness	Transverse stiffness	Longitudinal stiffness	Torsional stiffness	Rocking stiffness about Y	Rocking stiffness about Z
Value	1,391,158	1,517,895	7,517,895	1.57×10^7	9.7×10^6	9.7×10^6

Table 3. Bearing loads and rotations due to dead, live, brake and wind loads.

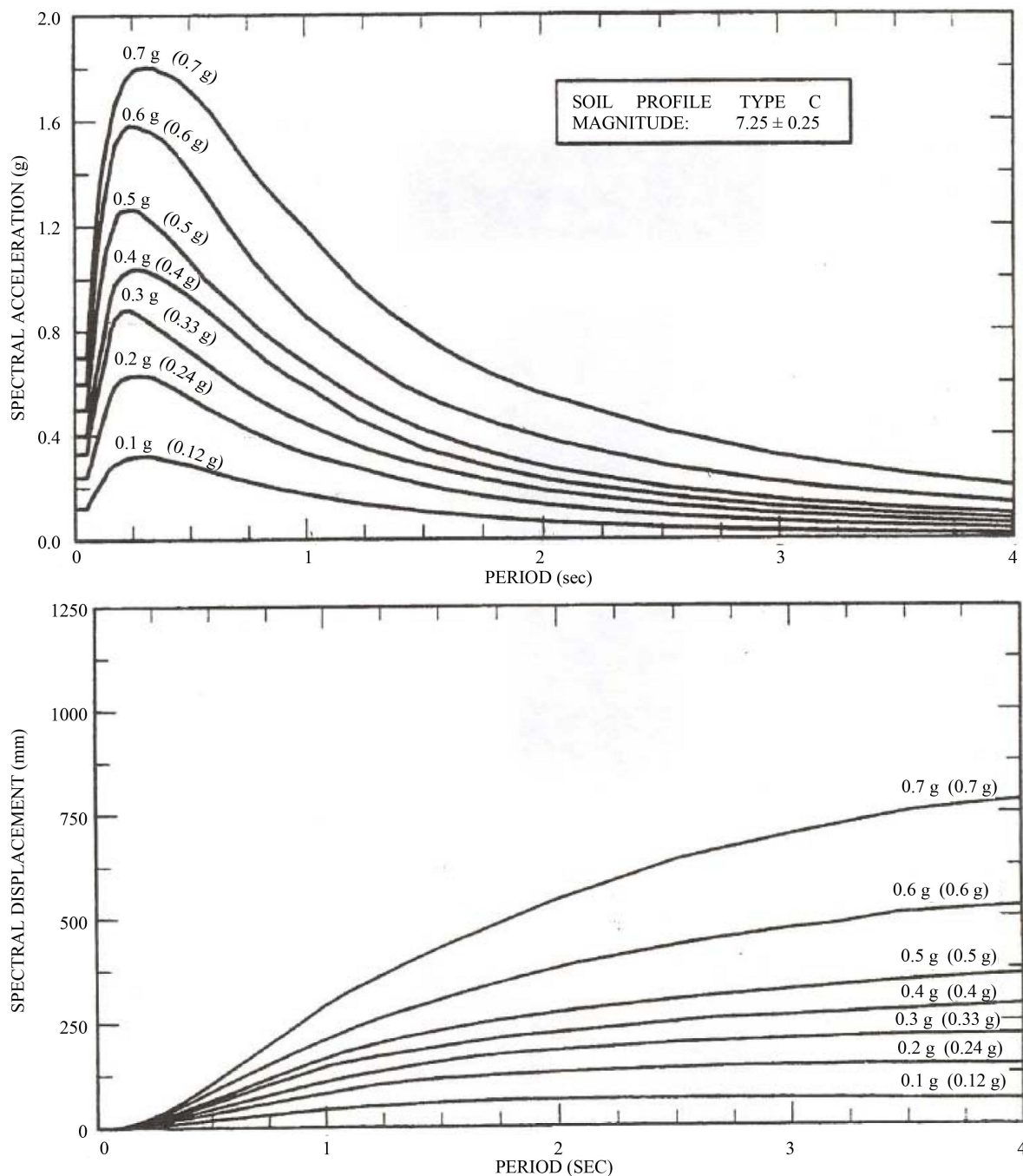
Loading	Abutment Bearings (per bearing)		Pier Bearings (per bearing)	
	Reaction (kN)	Reaction (rad)	Reaction (kN)	Reaction (rad)
Dead Load	V + 1497	0.00149	V + 4166	0.00006
Live Load (Truck, Tandem or Lane)	V + 610 V - 69	0.00057	V + 1101 V - 84	0.00040
HL93 (Live + IM + BR)	V + 835 V - 119	0.00090	V + 1550 V - 139	0.00064
Braking (BR)	V + 14 V - 14	0.00006	V + 18 V - 18	0.00004
Wind on Load (WL)	V + 11 V - 11 T 10	Negligible	V + 31 V - 31 T 29	Negligible
Wind on Structure (WS)	V + 12 V - 12 T 28	Negligible	V + 40 V - 40 T 90	Negligible
Vertical Wind on Structure (WV)	V - 142	Negligible	V - 458	Negligible

V: Vertical reaction; T: Transverse reaction; +: Compressive force; -: Tensile force.

2.2. Seismic Loading

Seismic loading is defined per Caltrans Seismic Design Criteria (2004) [6] to be the 5%-damped response spec-

trum of Magnitude 7.25, 0.7 g acceleration and soil profile C. The horizontal response spectra for acceleration and displacement are shown in **Figure 6**. This earthquake is considered to be the Maximum Earthquake. Calculations are performed only for this earthquake level and isolator safety checks are performed on the basis of the calculated response at this level. The vertical earthquake is assumed to be described by the spectra of **Figure 6** after multiplication by factor 0.70.



Note: Peak ground acceleration values not in parentheses are for rock (Soil Profile Type B) and peak ground acceleration values in parentheses are for Soil Profile Type C.

Figure 6. Horizontal 5%-damped response spectra for earthquake of magnitude 7.25 and soil profile type C (Adapted from Clatran Seismic Design Criteria (2004) [6]).

3. Design Analysis of Lead-Rubber Isolation System

This case study is developed as an alternative to the combined lead-rubber and elastomeric bearing isolation system (Constantinou, *et al.*, 2007 [7]). The combined system may not be desirable because two different isolator types are used in an application with only eight bearings. An all lead-rubber bearing system is simpler and requires less testing.

3.1. Single Mode Analysis

Criteria for applicability of single mode analysis are presented in **Table 4**. Kim (2007) [5] presents the calculations for the analysis and safety check of the isolation system. The all pier abutment and pier bearings are lead-rubber bearings with 200 mm diameter lead core. All bearings are of identical construction and of identical materials. Drawing of the bearings is shown in **Figure 7**. The bearings need not be installed pre-deformed in order to accommodate displacements due to post-tensioning and shrinkage. The bearings are safe for a service displacement of 75 mm (includes shrinkage and post-tensioning effects) and 455 mm seismic displacement.

Table 5 presents a summary of the calculated displacement and force demands, the effective properties of the isolated structure and the effective properties of each type of bearing. These properties are useful in response spectrum, multi-mode analysis. The effective stiffness was calculated using

$$K_{\text{eff}} = K_d + \frac{Q_d}{D_M} \quad (1)$$

where (a) for abutment bearing, $K_d = 1016 \text{ kN/m}$ and $Q_d = 234.85 \text{ kN}$ for lower bound and $K_d = 1439 \text{ kN/m}$ and $Q_d = 610.7 \text{ kN}$ for upper bound, and (b) for each pier bearing, $K_d = 1439 \text{ kN/m}$ and $Q_d = 313.1 \text{ kN}$ for lower bound and $K_d = 1439 \text{ kN/m}$ and $Q_d = 615.1 \text{ kN}$ for upper bound.

Table 4. Applicability criteria for methods of analysis.

Method of Analysis	Application Criteria
Single Mode	<ol style="list-style-type: none"> 1) Soil profile type A, B, C or D. 2) Bridge without significant curvature, defined as having a subtended angle in plan not more than 30°. 3) Effective period $T_{\text{eff}} \leq 4.0 \text{ sec}$. 4) Effective damping $\beta_{\text{eff}} \leq 0.30$. Method may be used when $\beta_{\text{eff}} > 0.30$ but less than 0.50 provided that $\beta_{\text{eff}} = 0.30$ is used. 5) Distance from active fault is more than 10 km. 6) The isolation system does not limit maximum displacement to less than the calculated demand. 7) The isolation system meets the re-centering capability criteria of Section 3.4 (Constantinou, <i>et al.</i>, 2007) [7].
Multimode	<ol style="list-style-type: none"> 1) Soil profile type A, B, C or D. 2) Bridge of any configuration. 3) Effective period $T_{\text{eff}} \leq 4.0 \text{ sec}$. 4) Effective damping $\beta_{\text{eff}} \leq 0.30$. Method may be used when $\beta_{\text{eff}} > 0.30$ but less than 0.50 provided that $\beta_{\text{eff}} = 0.30$ is used. 5) Distance from active fault >10 km. 6) The isolation system does not limit maximum displacement to less than the calculated demand. 7) The isolation system meets the re-centering capability criteria of Section 3.4 (Constantinou, <i>et al.</i>, 2007) [7].
Response History	<ol style="list-style-type: none"> 1) Applicable in all cases. 2) Required when distance to active fault is less than 10 km. 3) Required when soil profile type is E or F. 4) Required when $T_{\text{eff}} > 4.0 \text{ sec}$ or $\beta_{\text{eff}} > 0.50$. 5) Required when the isolation system does not meet there-centering capability criteria of Section 3.4 (Constantinou, <i>et al.</i>, 2007) [6], but it meets the criterion that the period calculated using the tangent stiffness of the isolation system at the design displacement is less than 6.0 sec.

Table 5. Applicability criteria for methods of analysis.

Parameter	Upper Bound Analysis	Lower Bound Analysis
Maximum Displacement D_M (mm) ¹	269	396
Total Maximum Displacement D_{TM} (mm) ²	N.A.	457.2
Base Shear/Weight	0.350	0.240
Abutment Bearing Seismic Axial Force (kN) ³	813.14	784.22
Pier Bearing Seismic Axial Force (kN) ³	2820.17	2786.81
Abutment Bearing Seismic Axial Force (kN) ⁴	524.00	307.37
Pier Bearing Seismic Axial Force (kN) ⁴	1124.96	1028.43
Effective Stiffness of Each Abutment Bearing K_{eff} (kN/m)	3730	1620
Effective Stiffness of Each Pier Bearing K_{eff} (kN/m)	3730	1810
Effective Damping	0.352	0.242
Damping Parameter B	1.800	1.660
Effective Period T_M (sec) (Substructure Flexibility Neglected)	1.76	2.58
Effective Period T_M (sec) (Substructure Flexibility Considered)	1.87	2.67

¹Based on one-directional excitation in longitudinal bridge direction; ²Based on three-directional excitation using 100% - 30% - 30% rule, and multiplying by Factor 1.1; ³Value is for 100% vertical + 30% transverse + 30% longitudinal combination (maximum axial load); ⁴Value is for 100% transverse + 30% vertical + 30% longitudinal combination (worst case for lead-rubber bearing safety check-combined with maximum bearing displacement).

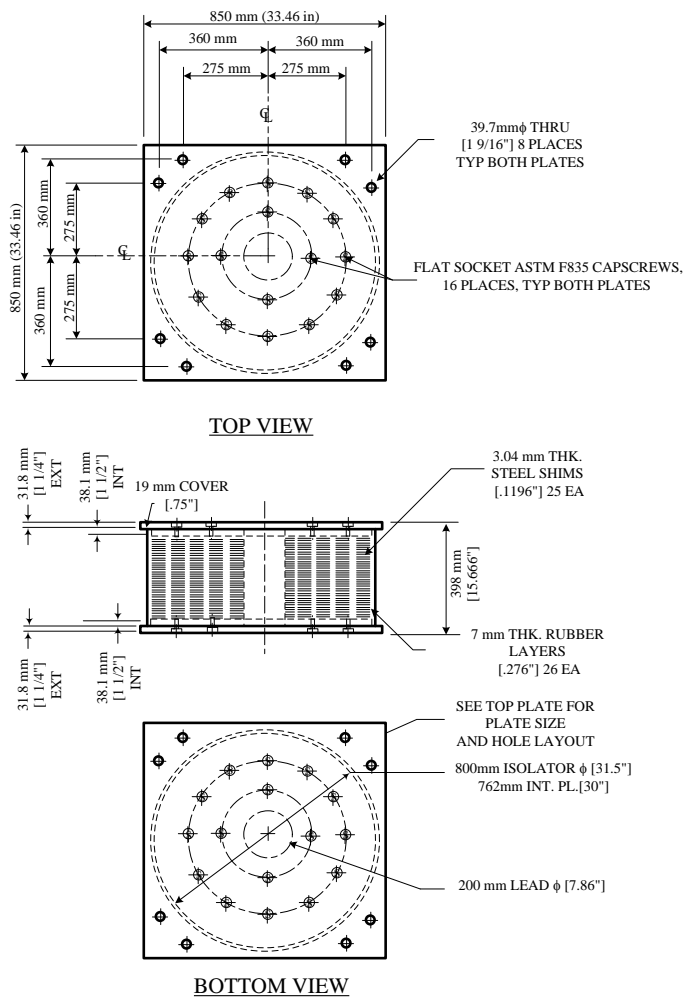


Figure 7. Principle structure and size of LRB for bridge example.

3.2. Multimode Response Spectrum Analysis

Figure 8 shows the bridge model used for response spectrum analysis. For this analysis, each isolator is modeled as a vertical 3-dimensional beam element-rigidly connected at its two ends-of length h , area A , moment of inertia about both bending axes I and torsional constant J . The element length is the height of the bearing, $h = 400$ mm (average height of bearings) and the area is calculated as described below in order to represent the vertical bearing stiffness. Note that the element is intentionally used with rigid connections at its two ends so that $P-\Delta$ effects are properly distributed to the top and bottom parts of the bearing. The vertical bearing stiffness was calculated using the theory presented in Section 9 of the report (Constantinou, *et al.*, (2007) [7]). Particularly, the vertical stiffness in the laterally un-deformed configuration is given by

$$K = \frac{A_r}{T_r} \left[\frac{1}{E_c} + \frac{4}{3K} \right]^{-1} \quad (2)$$

In Equation (2), T_r is total rubber thickness, T_r is the bonded rubber area (however adjusted for the effects of rubber cover by adding the rubber thickness to the rubber bonded diameter), K is the bulk modulus of rubber (assumed to be 2000 MPa). Moreover, E_c is the compression modulus given by

$$E_c = 6GS^2F \quad (3)$$

where G is the shear modulus of rubber, S is the shape factor and F is given by Equation (4) below with E_o and E_i being the outside and inside bonded diameters of the bearing. Note that for the calculation of the vertical stiffness of the lead-rubber bearing we consider that the lead core does not exist and treat the bearing as one without a hole for which parameter $F = 1$. Also, we used the nominal value of shear modulus G under static conditions in order to obtain a minimum value of vertical stiffness that can also be used in the bearing performance specifications.

$$F = \frac{\left(\frac{D_o}{D_i}\right)^2 + 1}{\left(\frac{D_o}{D_i} - 1\right)^2} + \frac{1 + \frac{D_o}{D_i}}{\left(1 - \frac{D_o}{D_i}\right) \ln \frac{D_o}{D_i}} \quad (4)$$

Torsional constant is set $J = 0$ or a number near zero since the bearing has insignificant torsional resistance. Moreover, shear deformations in the element are de-activated. The moment of inertia of each element is calculated by use of the following equation

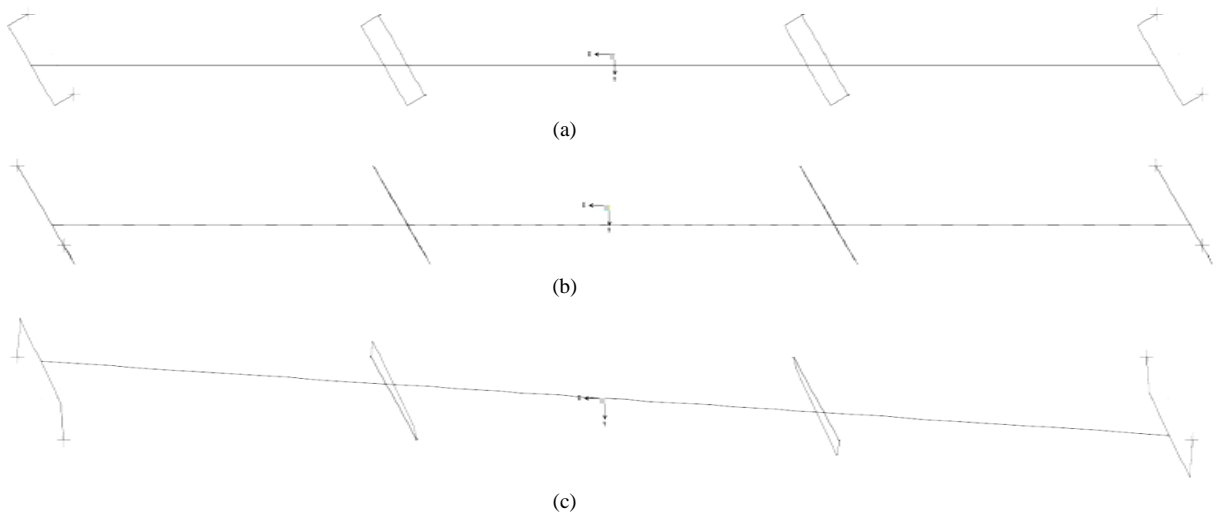


Figure 8. First three modes of vibration of isolated bridge with lead-rubber bearing system in lower bound analysis. (a) First mode: $T_1 = 2.67$ sec; (b) Second mode: $T_2 = 2.61$ sec; (c) Third mode: $T_3 = 2.21$ sec.

$$I = \frac{K_{\text{eff}} h^3}{12E} \quad (5)$$

Response spectrum analysis was performed using the response spectrum of **Figure 8** for 0.7 g which is 5%-damped spectrum after division by parameter B for periods larger or equal to $0.8 T_M$, where T_M is the effective period and B is the parameter that relates the 5%-damped spectrum to the spectrum at the effective damping. Quantities T_M , B and the effective damping are presented in **Table 5**. It should be noted that these quantities are given in **Table 5** for the upper and lower bound cases, both of which are analyzed. Values of $0.8 T_M$ are 1.3 sec for upper bound analysis and 2.0 sec for lower bound analysis. Values of parameters used in response spectrum analysis of lead-rubber bearing isolation system are presented in **Table 6**. Besides, values of spectral acceleration used in the analysis are presented in **Table 7**.

Eigenvalue and response spectrum analysis were performed in program SAP2000 [8]. **Figure 8** presents the mode shapes of the first three modes of vibration of the isolated bridge in the lower bound analysis. They are two modes dominated by translational displacements in two orthogonal directions, and a third torsional mode of vibration. The results are qualitatively the same as those for the combined lead-rubber and elastomeric bearing system with the first mode characterized by deformation of both the isolators and the piers along the weak direction of the pier. The period matches nearly exactly the period that is calculated in simplified analysis accounting for the effects of substructure flexibility ($T = 2.67$ sec). The second mode is deformation along the strong axis of the pier and accordingly it consists primarily of isolator deformation. This period matches nearly the period calculated neglecting the effect of substructure flexibility ($T = 2.58$ sec).

Analysis was performed by separately applying the earthquake excitation in the longitudinal, transverse and vertical bridge directions. The vertical response spectrum was taken as a 70% portion of the horizontal 5%-damped spectrum without any modification for increased damping.

The results of these analyses are presented in **Table 8** in terms of the bearing displacements; isolation shear force and bearing axial forces (only part due to earthquake). **Table 8** presents a comparison of key response quantities obtained by the single and multimode-response spectrum methods of analysis. In each type of analysis, quantity D_{TM} was calculated as the vectorial sum of bearing displacements due to longitudinal and transverse earthquake components combined using the 100% - 30% rule and then multiplying by Factor 1.1. The results demonstrate very good agreement in the calculated bearing displacement demands and isolation shear forces between the two methods of analysis.

Axial bearing forces are underestimated by the single mode analysis method due, primarily, to neglect of the skew in the calculations. Consideration of the skew angle is not difficult but the underestimation in the calculation of loads to have any significance in the safety of the bearings. Calculations show that the bearings have capacity to sustain the calculated loads in the maximum earthquake.

Table 6. Values of parameters h , A , I and E used in response spectrum analysis of lead-rubber bearing isolation system.

Bearing Location	Parameter	Upper Bound Analysis	Lower Bound Analysis
Abutment	Effective Horizontal Stiffness K_{eff} (kN/m)	3730	1620
	Vertical Stiffness K_v (kN/m)	1,760,000	1,760,000
	Height h (mm)	398.8	398.8
	Modulus E (MPa)	99,963	99,963
	Area A (mm ²)	6987	6987
Pier	Moment of Inertia I (cm ⁴)	19.5978	8.4982
	Effective Horizontal Stiffness K_{eff} (kN/m)	3730	1810
	Vertical Stiffness K_v (kN/m)	1,760,000	1,760,000
	Height h (mm)	398.8	398.8
	Modulus E (MPa)	99,963	99,963
	Area A (mm ²)	6987	6987
	Moment of Inertia I (cm ⁴)	19.5978	8.4982

Table 7. Spectral acceleration values used in response spectrum analysis of isolated bridge with lead-rubber bearing system.

Period T (sec)	Spectral Acceleration for 5%-Damping (g) [*]	Spectral Acceleration for Upper Bound Analysis (g)	Spectral Acceleration for Lower Bound Analysis (g)
0	0.70	0.70	0.70
0.05	0.70	0.70	0.70
0.10	1.29	1.33	1.33
0.24	1.77	1.78	1.78
0.30	1.80	1.80	1.80
0.50	1.72	1.75	1.75
0.75	1.44	1.44	1.44
1.00	1.19	1.19	1.19
1.25	0.95	0.95	0.95
1.40	0.86	0.48	0.86
1.50	0.78	0.43	0.78
1.60	0.72	0.40	0.72
1.75	0.64	0.36	0.64
2.00	0.55	0.31	0.55
2.10	0.53	0.29	0.32
2.20	0.50	0.28	0.30
2.50	0.41	0.23	0.25
2.75	0.37	0.21	0.22
3.00	0.32	0.18	0.19
3.25	0.29	0.16	0.17
3.50	0.25	0.14	0.15
3.75	0.23	0.13	0.14
4.00	0.20	0.11	0.12

*Vertical excitation spectrum is 0.7 times the 5%-damped horizontal spectrum.

Table 8. Key response quantities obtained by multimode analysis isolated bridge with lead-rubber bearing system.

Parameter	Upper Bound Analysis		
	100% Longitudinal EQ	100% Transverse EQ	100% Vertical EQ
Maximum Bearing Displacement, D_M (mm)	231.1 (P); 289.6 (A)	43.6 (P); 48.5 (A)	-
Isolation Shear/Weight	0.347	0.351	-
Bearing Axial Force (kN)	105.9 (P); 133.9 (A)	362.1 (P); 391.0 (A)	3226.3 (P); 1217.9 (A)
Parameter	Lower Bound Analysis		
	100% Longitudinal EQ	100% Transverse EQ	100% Vertical EQ
Maximum Bearing Displacement, D_M (mm)	355.6 (P); 406.4 (A)	373.4 (P); 398.8 (A)	-
Isolation Shear/Weight	0.234	0.236	-
Bearing Axial Force (kN)	50.0 (P); 61.8 (A)	230.0 (P); 251.8 (A)	3226.3 (P); 1217.9 (A)

Note: (P) denotes the pier bearings and (A) denotes the abutment bearings.

4. Conclusions

The examples presented in this paper demonstrate that single-mode and multi-mode analysis methods, when properly implemented, provide results in close agreement. On the basis of the results obtained in this study, the single mode method of analysis is sufficiently accurate and conservative to be used in analysis and design.

Examples of specifications which are consistent with the assumptions made in the analysis have been presented in this study. **Table 9** presents a summary of key response quantities for the two example designs of this paper as obtained by the single mode method of analysis. These quantities are the total maximum dis-

Table 9. Comparison of key response quantities for two examples as obtained by single mode method of analysis ($W = 22,650$ kN).

System	Lower Bound Analysis				Upper Bound Analysis			
	D_{TM} (mm)	F/W	F_a/W	F_p/W	D_M (mm)	F/W	F_a/W	F_p/W_p
Lead-Rubber and Elastomeric Bearing*	533	0.250	0.098	0.152	318	0.308	0.095	0.213
Lead-Rubber Bearing	457	0.240	0.113	0.127	269	0.350	0.175	0.175

*Constantinou, *et al.* (2007).

placement D_{TM} in the lower bound analysis, the maximum displacement D_T in the upper bound analysis, the base shear F/W and the portions of shear transmitted to the abutments, F_a/W , and piers, F_p/W , all normalized by the bridge weight $W = 22,650$ kN. The results demonstrate that the displacement demands in the two systems are about 457 to 533 mm. Brief summaries are as follows.

1) Total displacement ($D_{TM} = 457$ mm) on design for all Lead-Rubber bearings case is reduced comparing with combined lead-rubber and elastomeric bearing system ($D_{TM} = 533$ mm). As a result, this represents substantial reduction in cost because of reduction of expansion joint.

2) In lower bound analysis, the benefit of all LRB versus Elastomeric bearing/LRB is almost 2% reduction in shear force at pier. When F_p/W ratio is reduced, the force at pier is reduced by increasing stiffness.

3) Furthermore, while previous design requires tests for two types of bearing, another benefit is that construction and testing is needed to only one type of bearing.

Acknowledgements

The authors would like to gratefully acknowledge Professor Michael C. Constantinou for his advice to this study. This research was supported by research fund, Kumoh National Institute of Technology.

References

- [1] Constantinou, M.C., Whittaker, A.S., Kalpakidis, Y., Fenz, D.M. and Warn, G.P. (2006) Performance of Seismic Isolation Hardware under Service and Seismic Loading. Technical Report MCEER-07-0012, Multidisciplinary Center for Earthquake Engineering Research, State University of New York at Buffalo, Buffalo.
- [2] Berger/Abam Engineers, Inc. (1996) Federal Highway Administration Seismic Design Course, Design Example No. 4. (Document Available through NTIS, Document No. PB97-142111).
- [3] Federal Emergency Management Agency (2000) Prestandard and Commentary for the Seismic Rehabilitation of Buildings. FEMA 356, Washington DC.
- [4] American Institute of Steel Construction (AISC) (2001) Manual for Steel Construction, Load and Resistance Factor Design. 3rd Edition, American Institute of Steel Construction-AISC, Chicago.
- [5] Kim, W. (2007) Seismic Isolation of Bridges with Lead Rubber Bearings and Friction Pendulum Bearings with Viscous Dampers. State University of New York at Buffalo, Master Project Report, Buffalo.
- [6] California Department of Transportation (2004) Caltrans Seismic Design Criteria. Version 1.3. California Department of Transportation, Sacramento.
- [7] Constantinou, M.C., Whittaker, A.S., Fenz, D.M. and Apostolakis, G. (2007) Seismic Isolation of Bridges. Version 2, Report to Sponsor, California Department of Transportation, Sacramento.
- [8] CSI (2002) SAP 2000 Analysis Reference Manual. Computers and Structures Inc., Berkeley.

Scientific Research Publishing (SCIRP) is one of the largest Open Access journal publishers. It is currently publishing more than 200 open access, online, peer-reviewed journals covering a wide range of academic disciplines. SCIRP serves the worldwide academic communities and contributes to the progress and application of science with its publication.

Other selected journals from SCIRP are listed as below. Submit your manuscript to us via either submit@scirp.org or [Online Submission Portal](#).

